Bull. Korean Fish. Soc. 22(6), 375~384, 1990 韓水誌 22(6), 375~384, 1990

A Combined Effect of Differential Cooling and Topography on the Formation of Ulleung Warm Eddy

Young Ho SEUNG, Soo Yong NAM and Sang Yong LEE*

Department of Oceanography, Inha University, Incheon, 402-751, Korea

**Department of Oceanography, Pusan National University, Pusan 609-735, Korea*

A numerical experiment is made to study the combined effect of differential cooling and bottom topography on the formation of Ulleung Warm Eddy. The Ulleung Warm Eddy appears after the passage around the Ulleung Basin of coastal trapped baroclinic waves generated in the north initial density front to the north, the continental slopes both to the west and south, and the Yamato Rise to the east. It resides therefore always inside the Ulleung Basin, as confirmed by observations.

Introduction

Traditional hydrographic observations made by Fisheries Research and Development Agency have shown an accumulation of relatively warm water mass near Ulleung Island; this water mass will be named as Ulleung Warm Eddy or shortly UWE hereafter. The existence of UWE may be traced in layers from 100 *m* down to 400 *m* but seems to be most clear in layers of 200~300 *m* depth (e.g. Fig. 1). The presence of UWE seems to be a permanent feature but its location seems to vary slightly. Yearly variation of location can be seen in Na(1988).

How can the UWE be generated ? We first point out the fact that it always presents inside the Ulleung Basing; the Ulleung Basin is surrounded by continental shelves to the west and south and by Yamato Rise to the east(c.f. Fig. 2). So the bottom topography should play an important role. The usual way the topography affects the hydrography is through the dynamics of deep current. The Tsushima Warm Current (shortly TWC hereafter) entering the Korea Strait is confined to upper 100 *m* or so. It is therefore hard to expect that the TWC generates the deep current.

As pointed out by Manabe(1957), outbursts of cold and dry continental air from the northwest onto the Japan Sea in winter involve a large amount of heat flux from sea to atmosphere. It was shown that this air mass then undergoes a rapid transformation and acquire maritime characteristics when or even before they reach the Japanese coast. This means that oceanic cooling in winter is very strong in the upwind side(northwest) and rapidly weakens toward the downwind side(southeast). In this regard, the differential cooling may be an effective way of initiating the density-driven deep current in this region.

In this paper, we examine the formation process of the UWE by the combined effect of differential cooling and bottom topography.

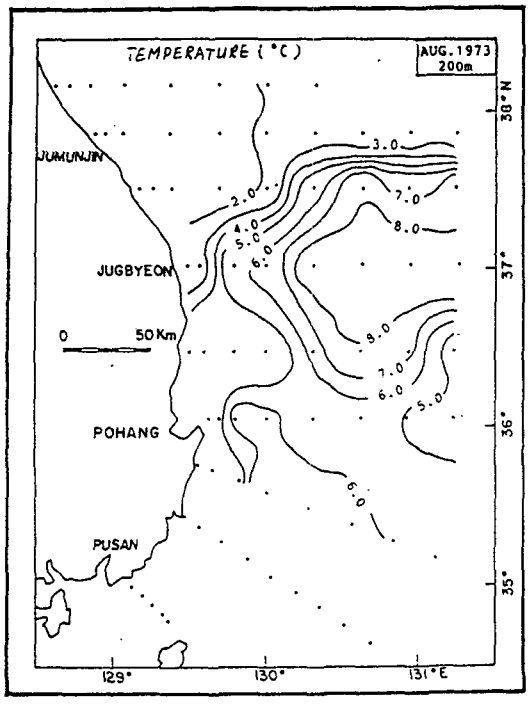

Fig. 1. An example of Ulleung Warm Eddy measured by Fisheries Research and Development Agency.

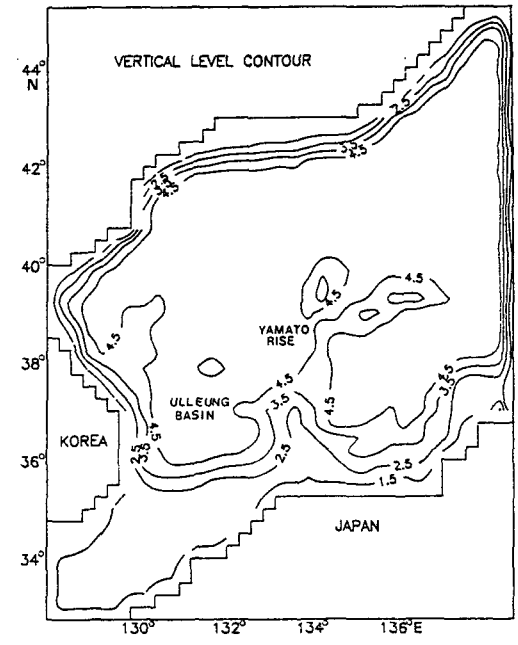

Fig. 2. Model domain with bottom topography. Depths are approximated as the number of levels counted from the surface. Isopleths shown are boundaries grouping the regions of same depth(in number of levels).

Numerical Experiment

To illustrate the combined effect of differential cooling and topography, a numerical experiment is performed using the Semtner(1974) version of Bryan-Cox's General Circulation Model. This is a multi-level model solving the primitive equations (see Appendix for equations and boundary conditions) and allowing the variable bottom topography. Five levels are taken here (see Table 1 for thickness of each layer). Grid size is a quarter degree of latitute and longitude and time step is 30 minutes. One thing should be mentions: because the grid size(about 25 *km*) is larger than the internal Rossby radius of deformation(shown to be about 16 *km* later), the length scale and phase speed of baroclinic waves in the numerical domain become somewhat larger and smaller, respectively, than the real ones(refer to Hsieh et al., 1983, for detailed discussions). Horizontal eddy diffusivity is taken as 5×10^6 $cm^2/$sec; horizontal eddy viscosity, 2×10^7 $cm^2/$sec; both vertical eddy diffusivity and viscosity, 1 $cm^2/$sec.

The numerical domain is the western part of the Japan Sea which includes a sufficiently large area around the Ulleung Basin-the area of interest in this study. Figure 2 shows the domain together with the bottom topography used in the model. Here, the depth is measured in number of levels counted from the surface. Even with 5-level vertical resolution, the characteristic topographic feature (Ulleung Basin and Yamato Rise etc.) is quite clearly seen. The open boundaries to the southwest and east are assumed closed. Justification of this assumption and limitation of the model results will be discussed later.

As mentioned earlier in Introduction, an intense winter-cooling occurs across the Japan Sea of which the intensity decreases rapidly toward the Japan side from the Continent side. This differential cooling will then create a horizontal density gradient. This gradient is dynamically unstable and an adjustment process generates ocean currents. In this paper, the differential cooling is idealized by

assuming two different regions: one with uniform cooling and the other without cooling. We note that this idealization does not reflect the reality. However, it may well give a physical insight and allow a qualitative estimation of the effect of differential cooling. The boundary between the two regions, which runs parallel to the latitute line of about 39 N, is therefore an initial density front. A "dam-breaking" experiment is made by removing the dam separating the two different water bodies. The Rossby adjustment process then takes place which evolves toward final steady state. During this process, deep motions are generated which are then affected by bottom topography. The initial density value of each level is given in Table 1. These values are referred to those observed along 102-line in summer and 106-line in winter, both in 1974, by Fisheries Research and Development Agency(1975). Different values of density may also be taken as long as these values can represent the cooling in the north.

The existence of artificial boundaries imposes some limitations in using the model. These boundaries prevent the flow of TWC which otherwise flows into the domain from the southwest. The TWC is not assumed to play an essential role in producting the UWE as discussed earlier in Introduction; however, a modifi-cation by the TWC is expected as discussed later.

In the Rossby adjustment process, both barotropic and baroclinic coastal trapped waves arise (Hsieh and Gill, 1984). These are generated at places where the closed boundaries meet the density front. These waves are trapped at, and travel along the boundary leaving the boundary on their right. Offshore scales of trapping are the Rossby Radius R for baroclinic, and the topographic length scale L for barotropic waves. For the density structure shown in Table 1, the first baroclinic mode(which contains most of baroclinic energy) has the maximum vertical motion between level 2 and 3. For the first mode, the Rossby Radius R is about 16 *km* in the south and about 6 *km* in the north of the initial front. Referring to the bathymetric chart(Fig. 2), L is of order 100 *km* in the south and negligibly small in the north of the initial front.

Effects of the artificial boundaries are therefore two fold: one occurs by offshore extension of the disturbances trapped against the artificial boundaries and the other occurs when these boundaries provide ways for disturbances to enter the region of interest(Ullenung Basin) causing contamination. The first effect can be ignored near the Ulleung Basin which lies sufficiently far from the artificial boundaries. In the second effect, the disturbances are trapped waves generated at the eastern edge of the front and traveling counterclockwise along the northern boundary. Phase speeds are fR(f= 10^{-4} sec^{-1} is the Coriolis parameter) for baroclinic, and fL for barotropic waves, which are equal to and smaller than, respectively, 50 *km*/day in the north of the initial front. Taking the peripheric distance from the eastern edge of the front to the Ulleung Basin as about 2,000 *km*, these waves will spend 40 days or more to travel this distance. This is much longer than the integration time of the model (25 days); we will see later that during 25 days the second effect mentioned above does not occur.

Table 1. Initial values taken at each level of the southern(S) and northern(N) part of the model domain.

Level	Thickness (meter)	Density(sigma-t) S/N
1	50	25.38/27.01
2	100	25.40/27.06
3	350	27.14/27.32
4	500	27.36/27.37
5	1,000	27.38/27.38

Results

The results are presented as follows: Figure 3 shows 5-day and 25-day density distributions at level 3; Figure 4 shows 5-day currents at level 2 for total(combined barotropic and baroclinic) and baroclinic currents; Figure 5 shows 25-day total currents at level 2 and 4; Figure 6 shows 25-day baroclinic currents at level 2 and 4. The density field(Fig. 3). indicates that baroclinic waves are generated at both ends of the initial density front

and propagate counterclockwise along the boundary. It also indicates that waves in the south is faster and more dispersed than those in the north. It seems that the topography(complex in the south and simple in the north) may play an important role here; in the north, distributions of both density(Fig. 3) and currents(Fig. 4 to 6) indicate that waves here are almost purely of baroclinic Kelvin type. Waves in the north travel so slowly that in 25 days they reach only to the northern end of the domain, confirming the assumption made earlier. However, baroclinic(Fig. 3) as well as barotropic(roughly estimated by subracting currents in Fig. 6 from in Fig. 5) waves in the south seem to have completed the trip along the southern boundary within 25 days.

Comparison of the 25-day density field with the topography(Fig. 2) indicates that baroclinic motions are trapped along the area of depth equivalent to first 3 levels(from the surface); the same comparison can be made between the 20-day baroclinic currents (Fig. 6) and the topography (Fig. 2). This fact can be easily understood when we realize that the first baroclinic mode can exist only for depth greater than first 3 levels and that these waves are coastally trapped; over the area with depth smaller than first 3 levels, barotropic currents will dominate(for rough estimation compare Fig. 5 and 6). The trapping of barotropic(over the area with depth of first 2-3 levels) and baroclinic(over the area with depth of first 3 levels) motions seem to weaken where the bottom slope is gentle.

Distributions of both density (Fig. 3) and baroclinic current (Fig. 6) suggest that baroclinic waves cannot move along the Yamato Rise; a very weak baroclinic motions are seen, however, in the north of the promotory of isobathic line 3.5(c.f. Fig. 2). It seems that the large curvature of isobathic lines (isobathic lines 2.5 and 3.5 in Fig. 2) cause scattering of waves.

The initial density front retains its mean position. It weakens slowly until a geostrophic balance is achieved across the front(compare Fig. 3 and Fig. 5 or 6). The center of the Ulleung Basin is left undisturbed and occupied by less dense water which may correspond to the UWE. There is another less dense water isolated inside the basin on the other side of the Yamato Rise. A dense water patch is also seen accumulated off the Japanese coast near 136 E, 36 N(Fig. 3). It is not clear wheather these are induced by the same baroclinic waves coming from the other side of the Yamato Rise.

Five days after the release of initial density discontinuity, currents are mostly in transient state though the barotropic component alone seems to be in the steady state to the south(Fig. 4). It is reminded that the steady state is established only after the passage of the wave fronts. Since the barotropic waves are much faster, barotropic field becomes steady first. After 25 days, the most energetic baroclinic component has also completed its journey around the southern basin and conditions become nearly in steady state here; furthermore, comparison of the 25-day density field (Fig. 3) and the vertical shear of 25-day current (see Fig. 5; the vertical shear is more clearly seen in the baroclinic current structure such as those in Fig. 6) indicate that motions are nearly in geostrophic balance. At this time, the UWE involves an anticyclonic circulation of the upper layer waters overlying the nearly motionless lower layer waters.

Discussion and Conclusions

The UWE produced in this experiment is not complete because we emphasized only the effects of cooling and topography. Major discrepancies may be arisen by ignoring the effect of incoming TWC. Though it is not essential in producing the UWE, the TWC can modify the local density field around its path. Assuming the geostrophy of TWC, less dense water will accumulate on the right of the TWC looking downstream. The model-produced density field seems to show an overestimation of density gradient in the south and an underestimation in the east of UWE. The currents along the southern continental slope of the model basin are unrealistic too. Referring to previous works, though without topography, such as that by Yoon(1982), it seems that these discrepancies are due to the neglect of TWC. In fact, these unrealistic features occuring along the southern continental slope will

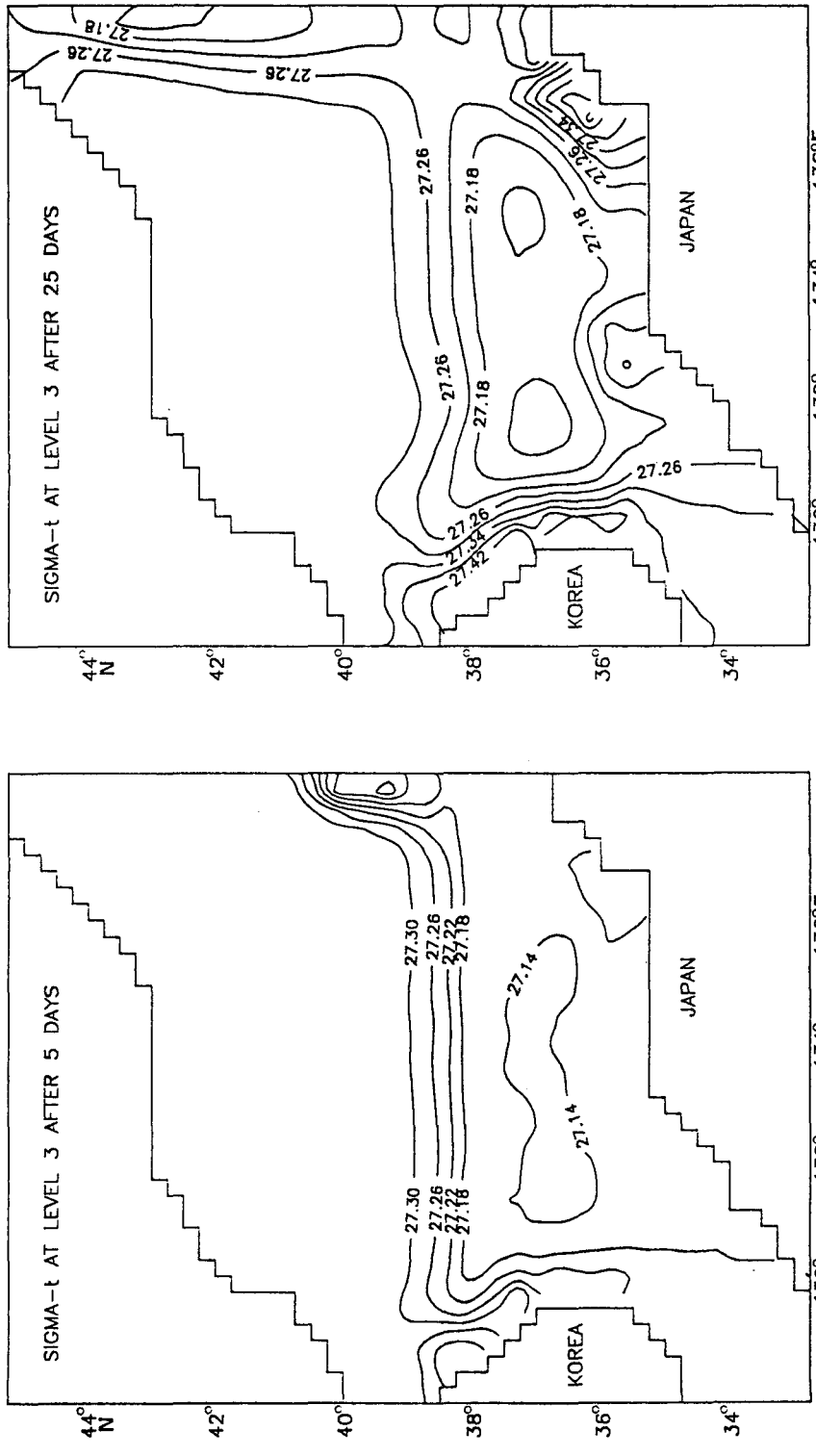

Fig. 3. Horizontal density distributions at level 3 after 5 days and 25 days. Note the appearence of a warm(less dense) eddy isolated inside the Ulleung Basin.

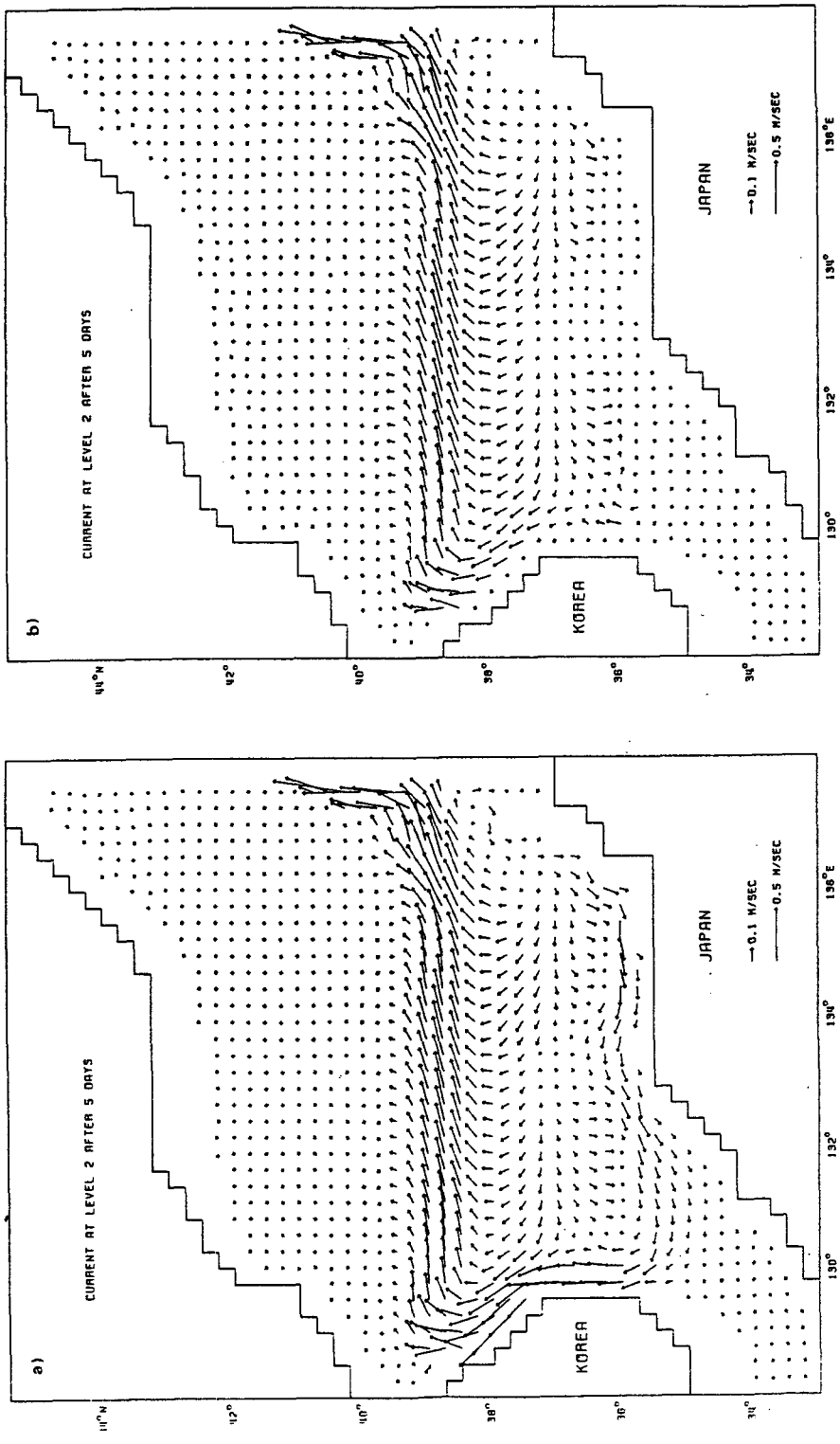

Fig. 4. Combined barotropic and baroclinic (a), baroclinic (b) currents after 5 days at level 2.

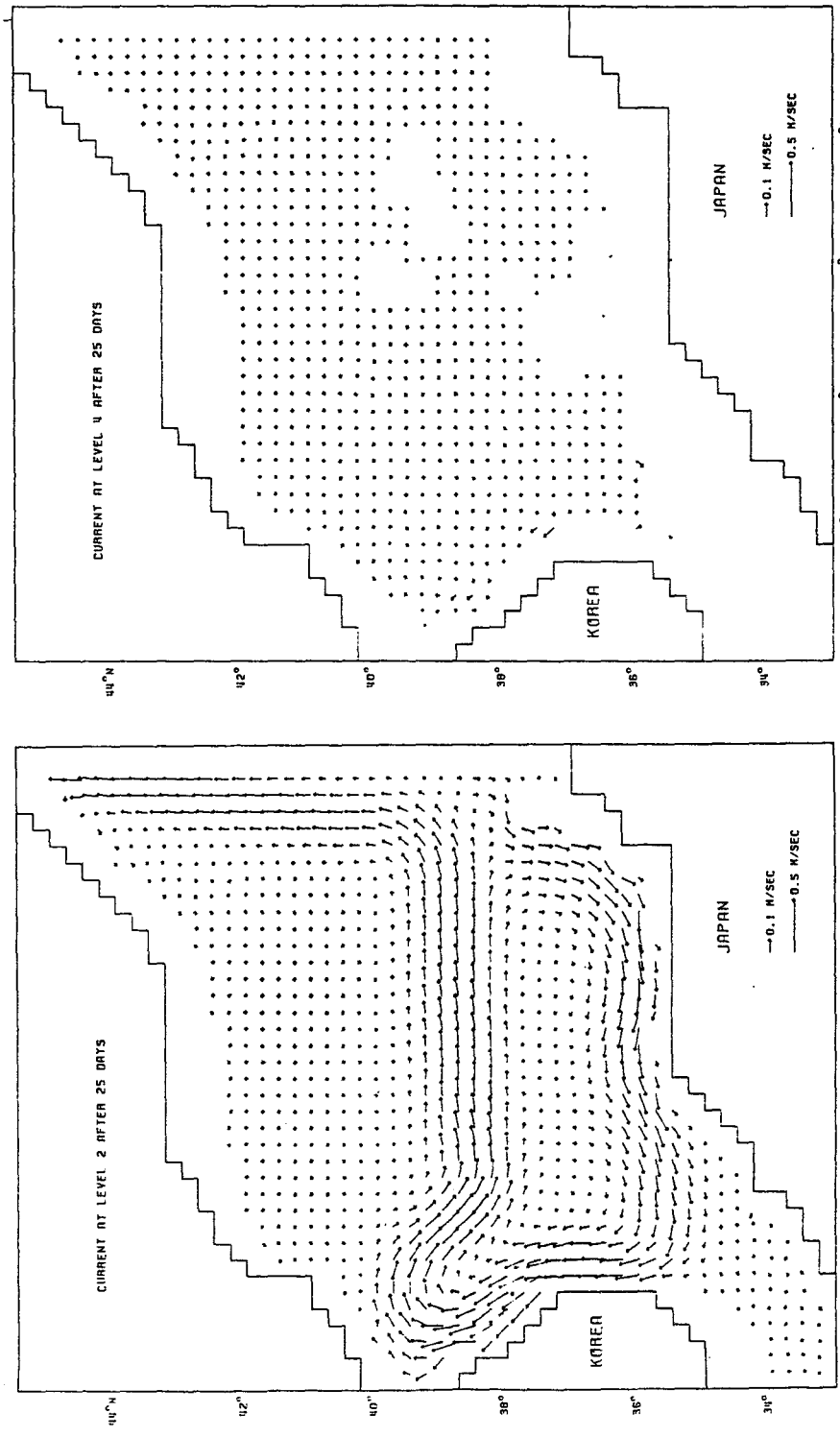

Fig. 5. Combined barotropic and baroclinic currents after 25 days at level 2 and 4. Note the anticyclonic circulation at level 2.

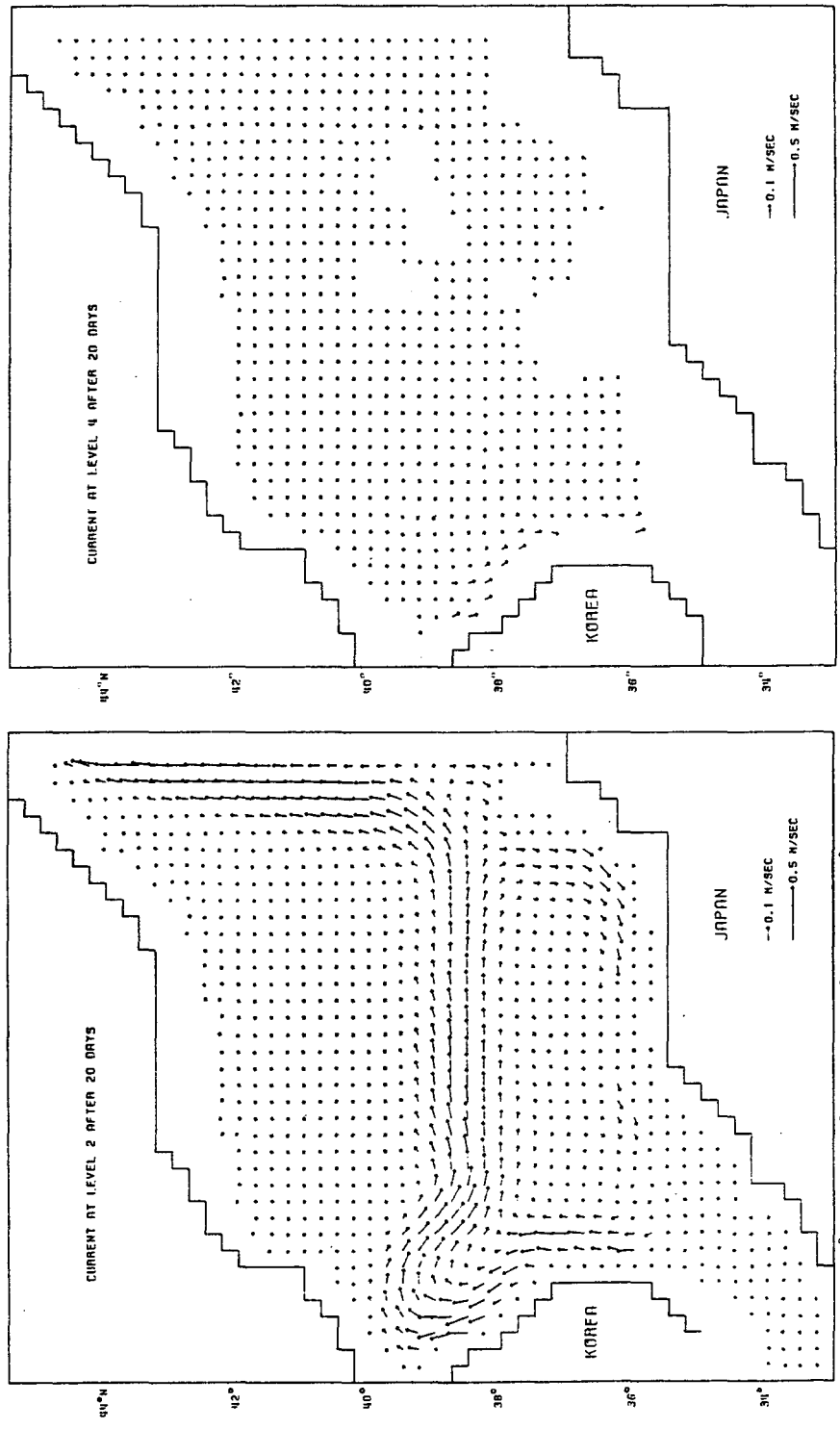

Fig. 6. Baroclinic currents after 20 days at level 2 and 4. Note the anti-cyclonic circulation at level 2.

disappear when the TWC flowing eastward is imposed.

Despite some limitations and the oversimplification of the model, we conclude that the combined effect of differential cooling and bottom topography can be an essential factor in producing the UWE, unless we admit the existence of the anti-cyclonic wind system over the Ulleung Basin or the UWE (Na, 1988). The extension of UWE is bounded by the initial density front to the north, the continental slopes to the west and south the Yamato Rise to the east, i.e., it locates inside the Ulleung Basin as observations indicate. The modification due to the passage of TWC will be an interesting subject in its own right and should be considered for more complete study.

Acknowledgements

* This study was supported in part by the Basic Sciences Research Institute Program, Ministry of Education, 1988. Contribution No. 251 of Institute of Marine Sciences, National Fisheries University of Pusan.

The author thanks to an anonymous referee for his kind corrections and comments.

References

Fisheries Research and Development Agency, 1975. Annual Report of Oeanographic Oservations, 23. Pusan, Korea.

Hsieh, W. W., M. K. Davey and R. C. Wajsowicz, 1983. The free Kelvin wave in finite-difference numerical models. J. Phys. Oceanogr., 13, 1383~1397.

Hsieh, W. W. and A. E. Gill, 1984. The Rossby Adjustment problem in a rotating, stratified channel with and without topography. J. Phys. Oceanogr., 14, 424~437.

Manabe, S., 1957. On the modification of air-mass over the Japan Sea when the outburst of cold air predominates. J. Met. Soc. Japan, Ser. II. 35, 311~326.

Na, J. Y., 1988. Wind stress distribution and its application to the upper-layer structure in the East Sea of Korea. J. Oceanol. Soc. Korea, 23, 97~109.

Semtner, A. J., 1974. An oceanic general circulation model with bottom topography: Numerical simulation of weather and climate, Tech Rep. No. 9. Univ. of Calif., Los Angeles. 99pp.

Yoon, J. H., 1982. Numerical experiment on the circulation in the Japan Sea Part I. Formation of the East Korean Warm Current. J. Oceanogr. Soc. Japan, 38, 43~51.

Appendix

Take the earth to be a sphere of radius a. A spherical coordinate system is used with λ, φ, and z representing longitude, latitude, and height. The ocean is contained between the surface $z=0$ and the bottom $z=-H(\lambda, \varphi)$. There velocity components are (u, v, w) in (λ, φ, z) directions. Other variables are pressure p and density ρ. The ocean is incompressible and has constant eddy viscosity coefficient κ and A_M in the vertical and horizontal directions respectively. It also has constant eddy diffusivity coefficient κ, and A_H in the vertical and horizontal directions. The governing equations of the model take the hydrostatic and Boussinesq approximations. In the horizontal momentum equations, the viscous and Coriolis' forces are neglected. The equations are:

$$\frac{\partial u}{\partial t} + Lu - \frac{uv\tan\varphi}{a} - fv = -\frac{1}{\rho_0 a\cos\varphi}\frac{\partial \varphi}{\partial \lambda} + \kappa\frac{\partial^2 u}{\partial z^2} + A_M\left\{\nabla^2 u + \frac{(1+\tan^2\varphi)u}{a^2} - \frac{\alpha\sin\varphi}{a^2\cos^2\varphi}\frac{\partial v}{\partial \lambda}\right\}$$

$$\frac{\partial v}{\partial t} + Lv + \frac{u^2\tan\varphi}{a} - fu = -\frac{1}{\rho_0 a}\frac{\partial \rho}{\partial \varphi} + \kappa\frac{\partial^2 v}{\partial z^2} + A_M\left\{\nabla^2 v + \frac{(1-\tan^2\varphi)v}{a^2} + \frac{\alpha\sin\varphi}{a^2\cos^2\varphi}\frac{\partial u}{\partial \lambda}\right\},$$

$$\frac{\partial \rho}{\partial z} = -\rho g,$$

$$\frac{1}{a\cos\varphi}\frac{\partial u}{\partial\lambda}+\frac{1}{a\cos\varphi}\frac{\partial}{\partial\varphi}(v\cos\varphi)+\frac{\partial w}{\partial z}=0,$$

$$\frac{\partial e}{\partial t}+L\rho=\kappa\frac{\partial^2\rho}{\partial z^2}+A_H\nabla^2\rho,$$

In the above, we have the advection operater,

$$L(\sigma)=\frac{1}{a\cos\varphi}\frac{\partial}{\partial\lambda}(u\sigma)+\frac{1}{a\cos\varphi}\frac{\partial}{\partial\varphi}(\cos\varphi\, v\sigma)+\frac{\partial}{\partial z}(w\sigma)$$

and f is the Coriolis' parameter varying with latitude.

Boundary conditions taken at both the ocean surface and bottom are those of no flux of momentum and density:

$$\left.\begin{aligned}\rho_o\kappa\frac{\partial}{\partial z}(u, v)&=0\\ \rho_o\kappa\frac{\partial}{\partial z}(T, S)&=0\end{aligned}\right\}\quad \text{at } z=0$$

$$\left.\begin{aligned}\rho_o\kappa\frac{\partial}{\partial z}(u, v)&=0\\ \rho_o\kappa\frac{\partial}{\partial z}(T, S)&=0\end{aligned}\right\}\quad \text{at } z=-H(\lambda, \varphi)$$

At lateral walls, no-slip conditions are imposed, u =v=0, and no-flux of heat or salt is allowed in the same way as the conditions at the surface and bottom are applied. The surface of the ocean is assumed a rigid lid. At the ocean bottom the flow is required to be parallel to the slope:

$$\omega=-\frac{u}{a\cos\varphi}\frac{\partial H}{\partial\lambda}-\frac{v}{a}\frac{\partial H}{\partial\varphi}\quad \text{at } z=-H(\lambda, \varphi)$$

Received December 20, 1989
Accepted January 20, 1990